Common Features in the Crystal Structures of the Compounds Bis(dimethylstibanyl)oxane and -sulfane, and the Minerals Valentinite and Stibnite (Grauspießglanz)

H. J. Breunig*, E. Lork, R. Rösler

Bremen, Institut für Anorganische und Physikalische Chemie der Universität Bremen

G. Becker*, O. Mundt, W. Schwarz

Stuttgart, Institut für Anorganische Chemie der Universität Stuttgart

Received March 20th, 2000.

Dedicated to Professor Ulrich Müller on the Occasion of his 60th Birthday

Abstract. Bis(dimethylstibanyl)oxane (**1**) and -sulfane (**2**), the two simplest organoelement species with an Sb–E–Sb fragment (E = O, S), were prepared by alkaline hydrolysis of bromodimethylstibane and by oxidation of tetramethyldistibane with sulfur [18], respectively. As shown by an x-ray structure analysis of compound **1** (m. p. $< -20\,°C$; $P2_12_12_1$, $a = 675.9(2)$, $b = 803.1(2)$, $c = 1666.8(4)$ pm at $-70 \pm 2\,°C$; $Z = 4$; $R1 = 0.042$), the molecules (O–Sb 198.8 and 209.9 pm, Sb–O–Sb 123.0°) adopt a *syn-anti* conformation in the solid state and are arranged in zigzag chains along [010] via weak intermolecular O··Sb interactions (258.5 pm, Sb–O··Sb 117.8°, O··Sb–O 173.5°) making use, however, of only one Me_2Sb moiety. Primary and secondary bond lengths and angles agree very well with corresponding values published for valentinite, the orthorhombic modification of antimony(III) oxide [3]. Bis(dimethylstibanyl)sulfane (**2**) (m. p. 29 to 31 °C) crystallizes in the uncommon space group $P6_522$ ($a = 927.8(3)$, $c = 1940.9(7)$ pm at $-100 \pm 2\,°C$; $Z = 6$; $R1 = 0.021$). Owing to coordination numbers of (1 + 1) and (2 + 2) for both Me_2Sb groups and the sulfur atom, respectively, molecules with an approximate *syn-syn* conformation (S–Sb 249.8 pm, Sb–S–Sb 92.35°) build up a three-dimensional net of double helices which are linked together by Sb··S contacts (316.4 pm). These parameters shed more light onto the rather complicated structure and bonding situation in stibnite (antimony(III) sulfide [4]). The molecular packing of compound **2** is compared with the structures of relevant inorganic solids, especially with that of *β*-quartz [37].

Keywords: Antimony compounds; *Bis(dimethyl*stibanyl)oxane; *Bis(dimethyl*stibanyl)sulfane; Crystal structure; Valentinite; Stibnite; Bond-valence analyses

Gemeinsamkeiten in den Kristallstrukturen der Verbindungen Bis(dimethylstibanyl)oxan und -sulfan und den Mineralien Valentinit und Stibnit (Grauspießglanz)

Inhaltsübersicht. Bis(dimethylstibanyl)oxan (**1**) und -sulfan (**2**), die beiden einfachsten elementorganischen Vertreter mit einer Sb–E–Sb-Einheit (E = O, S) wurden durch alkalische Hydrolyse von Bromdimethylstiban bzw. durch Oxidation von Tetramethyldistiban mit Schwefel [18] dargestellt. Nach den Ergebnissen einer Röntgenstrukturanalyse an Verbindung **1** (Schmp. $< -20\,°C$; $P2_12_12_1$, $a = 675{,}9(2)$, $b = 803{,}1(2)$, $c = 1666{,}8(4)$ pm bei $-70 \pm 2\,°C$; $Z = 4$; $R1 = 0{,}042$) nehmen die Moleküle (O–Sb 198,8 und 209,9 pm; Sb–O–Sb 123.0°) im Festkörper die *syn-anti* Konformation ein und ordnen sich unter Beteiligung nur einer der beiden Me_2Sb-Gruppen über kurze intermolekulare O··Sb Kontakte (258,5 pm; Sb–O··Sb 117,8°; O··Sb–O 173,5°) zu Zickzack-Ketten längs [010] an. Ähnliche Bindungslängen, -winkel und Kontakte treten in der bekannten Kristallstruktur des Minerals Valentinit, der orthorhombischen Modifikation des Antimon(III)-oxids [3], auf. Bis(dimethylstibanyl)sulfan (**2**) (Schmp. 29 bis 31 °C) kristallisiert in der verhältnismäßig seltenen Raumgruppe $P6_522$ ($a = 927{,}8(3)$, $c = 1940{,}9(7)$ pm bei $-100 \pm 2\,°C$; $Z = 6$; $R1 = 0{,}021$). Mit Koordinationszahlen von (1 + 1) für nun alle Me_2Sb-Gruppen bzw. (2 + 2) für die Schwefelatome bauen die annähernd *syn-syn* konformierten Moleküle (S–Sb 249,8 pm; Sb–S–Sb 92,35°) über Sb··S Kontakte (316,4 pm) eine dreidimensional verknüpfte Anordnung von Doppelhelices auf. Mit den an Verbindung **2** bestimmten Werten lassen sich entsprechende Parameter aus der verhältnismäßig komplizierten und bindungstheoretisch schwer verständlichen Struktur des Minerals Stibnit (Grauspießglanz, Sb_2S_3 [4]) gut einordnen. Die Packung der Bis(dimethylstibanyl)sulfan-Moleküle wird mit einigen im Aufbau ähnlichen anorganischen Festkörpern, insbesondere aber mit *β*-Quarz [37] verglichen.

---

* Prof. Dr. H. J. Breunig
Institut für Anorganische und
Physikalische Chemie
der Universität Bremen
Fachbereich 2
D-28334 Bremen

Prof. Dr. G. Becker
Institut für Anorganische Chemie
der Universität Stuttgart
Pfaffenwaldring 55 (Stgt.-Vaihingen)
D-70569 Stuttgart

Introduction

As a continuation of our studies on distibanes and related compounds [1], which to a considerable extent display intermolecular associations in the solid state, we were interested to learn more about the structures of distibanyl chalcogenanes in different states of aggregation. It would be of particular interest if structural features, which are typical for the different modifications of antimony(III) oxide [2, 3] and sulfide [4–10], can also be recognized in the solid state of simple species like the methyl derivatives $(Me_2Sb)_2O$ (**1**) and $(Me_2Sb)_2S$ (**2**). With respect to bis(dimethylstibanyl)-sulfane (**2**) especially, these studies are expected to bring forth a deeper insight into the rather complicated structure of stibnite (Grauspießglanz); for this black (or grey) modification of antimony(III) sulfide the results of several crystal structure determinations in space group *Pnma*, carried out at ambient temperature, were reported [4].

In this context one should emphasize that research on the modifications of antimony(III) sulfide is still being continued. To begin with, the structure of synthetic stibnite was redetermined by *Łukaszewicz* et al. [5] at 320 K on the basis of the acentric space group *Pmn*2_1, since physical properties such as the dielectric permittivity and the pyroelectric effect had been interpreted to indicate diffuse phase transitions at about 420 and 300 K as well as the absence of a center of symmetry at lower temperatures in both natural and melt-grown crystals of antimony(III) sulfide, respectively. However, with regard to space group *Pnma* only an insignificant improvement of the *R*-index from 0.0311 to 0.0301 could be achieved. One year before, a completely different, previously unknown structure had been published [6] for a mineral from Andra Pradesh, India, which, remarkably, crystallizes in dark grey needles as well. Heating a coprecipitate of antimony(III) oxide and sulfide with a saturated solution of sodium carbonate in a sealed tube for three days at 250 °C resulted in the formation of a few bronze-colored crystals; the x-ray structure analysis revealed that the compound $Sb_{10}S_{15}$, a lead-free analogue of the mineral fülöppite ($Pb_3Sb_8S_{15}$), had been isolated [7]. Without doubt, from a structural as well as a preparative point of view both results do need a detailed substantiation. Furthermore, it has been reported [8] that the diffraction patterns of commercially available orange antimony(III) sulfide do not match that obtained from the black modification. Finally, elucidating the structure of the orange form, which is precipitated by hydrogen sulfide from aqueous solutions, turned out to be extremely difficult [9, 10].

In preceding publications [11–13] the structures and conformational preferences of the gaseous molecules $(Me_2Sb)_2O$ (**1**) and $(Me_2Sb)_2S$ (**2**) and of the congenerous selenium and tellurium compounds as determined by gas electron diffraction (GED) and density functional theory (DFT) calculations were reported. In order to describe the different conformations of these molecules, the torsional angles Ep–Sb–E–Sb, where Ep stands for the assumed direction of the lone pair at antimony and E for oxygen or sulfur, were used; these parameters are easily calculated from the corresponding pairs of torsional angles C–Sb–E–Sb (Table 3). With an assignment of the expressions *syn* and *anti* to angles of 0° and 180°, the extreme molecular conformations of compounds **1** and **2** are *syn-syn* and *syn-anti*, i. e. C_{2v} and C_s symmetry, respectively (Scheme 1).

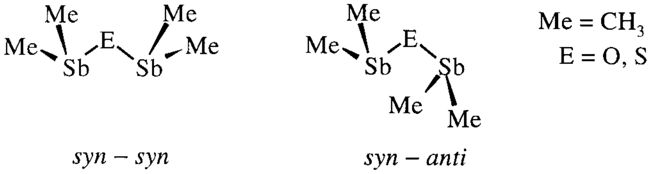

Scheme 1

DFT calculations on compounds **1** and **2** revealed that molecules with a conformation strictly or near *syn-syn* (Ep–Sb–E–Sb < 45°) are in an extremely flat minimum of energy; the *syn-anti* conformer was found to be higher in energy by only 4.6 and 3.9 kJ mol^{-1}, respectively. In agreement with these results, the presence of both conformers in the gas phase had to be assumed in structure determinations from electron diffraction data; the mole fractions of the *syn-syn* conformers were refined to values of 0.49(7) and 0.52(4) for bis(dimethylstibanyl)oxane (**1**) and -sulfane (**2**), respectively [11, 12].

Now we report the results of crystal structure analyses of compounds **1** and **2** and discuss structural features that are in common with the organoelement species and the inorganic solids valentinite and stibnite. Since knowledge of the atomic arrangements in these two minerals is not believed to be widespread, for a better comparison elaborate representations of the crystal structures and detailed descriptions are given in order to substitute abstract projections and simplified figures which are found in previous publications ([3, 4]; [10], p. 239) and monographs [14–16].

Experimental Section

Preparation. Bis(dimethylstibanyl)oxane (**1**) was first isolated in 1925 by *Morgan* and *Davies* [17] as a colorless oil from an alkaline hydrolysis of bromodimethylstibane, but unfortunately preparative details were reported only very briefly by the authors. It is also formed as an intermediate, which undergoes further oxidation, when tetramethyldistibane is exposed to air [18]. We synthesized compound **1** at ambient temperature by adding freshly prepared bromodimethylstibane to an aqueous solution of sodium hydroxide (eq. (1)) and extracting the crude product with petroleum ether. After repeated distillation it was obtained in 60% yield as a colorless liquid that ignites in air. The maximum purity of only 98.5% is attributed mainly to traces of trimethylstibane, which was already the major by-product in the starting material Me_2SbBr. Compound **1** solidifies at a temperature just below –20 °C; it shows a medium solubility in water, is miscible with many organic solvents and forms azeotropes with tetrahydrofuran and diethyl ether. However, we cannot confirm the description of bis(dimethylstibanyl)oxane (**1**) as a white, microcrystalline solid that is stable towards oxidation [19].

$$2\,Me_2Sb\text{–}Br + 2\,OH^- \xrightarrow{<H_2O>} \underset{\mathbf{1}}{(Me_2Sb)_2O} + 2\,Br^- + H_2O \qquad (1)$$

The congenerous compound **2** was obtained from the previously reported oxidation of tetramethyldistibane with sulfur in benzene at 25 °C (eq. (2)) [18]; the colorless liquid isolated in 96% yield solidifies to give yellow crystals with a melting point of 29 to 31 °C. Exposure to light results in the formation of trimethylstibane and yellow resinous products; this decomposition is particularly rapid in organic solvents.

$$Me_2Sb\text{–}SbMe_2 + {}^1/_8\,S_8 \xrightarrow{<C_6H_6>} \underset{\mathbf{2}}{(Me_2Sb)_2S} \qquad (2)$$

Bis(dimethylstibanyl)oxane (**1**) and -sulfane (**2**) are both extremely malodorous compounds; hence the trivial names antimony-cacodyl oxide and sulfide are fully justified. Until now the knowledge of their chemical reactivity was rather poor; however, recent investigations by some of us [20] on the behavior of these molecules versus tetracarbonyl(norbornadiene)chromium resulted in the isolation of the cyclic complexes $[\mu_2\text{-}(Me_2Sb\text{–}E\text{–}SbMe_2)(OC)_4Cr]_2$ (E = O, S) and their characterization by x-ray structure analyses. Additionally, bis(dimethylstibanylsulfanyl)(methyl)stibane, one of the decomposition products of compound **2**, could be trapped as the chelate complex $[MeSb(\text{–}S\text{–}SbMe_2)_2](OC)_4Cr$.

Crystal Growth. Colorless single crystals of compound **1** were obtained in a quartz capillary of 0.3 mm diameter utilizing the commercially available crystal growing device CR-LK93 of COMRAY Analytics GmbH, D-42553 Velbert. The sample was sealed, mounted on the diffractometer and cooled to a temperature of –70 ± 2 °C which is sufficiently far below the melting point. Subsequent zone melting was accomplished by moving the beam of a CO_2 laser gradually up and down the sample; its intensity had to be adjusted such as to liquify a small cylindrical section only. By this procedure a single crystal of appropriate length and quality could be grown fairly easily. Owing to a higher melting point, suitable crystals of compound **2** were already formed on cooling the melt slowly.

Data Collections and Structure Refinements. Automated centering of 25/27 selected reflections in a range of $15° < \theta < 18°/8° < \theta < 13°$ and least-squares routines were employed to obtain the cell parameters of compounds **1** and **2**. The results as well as details of data collections and structure refinements are summarized in Table 1. From the dimensions of the unit cell, additional *E*-value statistics and systematic absences the correct space group $P2_12_12_1$ was derived for bis(dimethylstibanyl)oxane (**1**). In the case of the sulfur compound **2** the choice of the pair $P6_122/P6_522$ over $P6_1/P6_5$ was decided during the course of the structure refinement. Furthermore, for the crystal under inspection the assumption of space group $P6_522$ could be justified by an absolute structure parameter of 0.01(7) and an *R*1-index of 0.0211 – in contrast to corresponding results of 1.00(8) and 0.0223 obtained with space group $P6_122$.

After the usual Lp-corrections, phases were determined with statistical methods and the structures were refined on F^2 with full-matrix least-squares methods, utilizing the program system SHELX-97 [21 d] and complex scattering factors of the neutral atoms [21 e, f] as included therein. Finally, when individual anisotropic displacement parameters to all

Table 1 Summary of crystal data, details of data collections and results of structure refinements for compounds **1** and **2**

	1	**2**
empirical formula	$C_4H_{12}OSb_2$	$C_4H_{12}SSb_2$
CAS registry number	[73513-49-2]	[84372-76-9]
formula mass (g mol^{-1})	319.64	335.70
melting point (°C)	< –20	29 to 31
space group	$P2_12_12_1$ (N° 19 [21 a])	$P6_522$ (N° 179 [21 a])
unit cell dimensions (pm)	$a = 675.9(2)$ $b = 803.1(2)$ $c = 1666.8(4)$	$a = 927.8(3)$ $c = 1940.9(7)$
cell volume (10^{-30} m^3)	904.8	1446.9
Z (molecules)	4	6
calc. dens. ρ (10^3 kg m^{-3})	2.346	2.312
F(000)	584	924
abs.coeff. μ (10^2 m^{-1}) [21 b]	5.891	5.733
crystal size (mm)	column of 0.3 mm diameter	0.8 × 0.7 × 0.4
diffractometer	Siemens P3	Siemens P4
radiation (pm)	Mo$K\alpha$ (71.073)	Mo$K\alpha$ (71.073)
temperature (°C)	–70 ± 2	–100 ± 2
scan type	Wyckoff	$\omega/2\theta$
θ range	2.44° to 30.05°	2.53° to 27.52°
index ranges	$0 \le h \le 9$; $0 \le k \le 11$; $-1 \le l \le 23$	$-1 \le h \le 11$; $-12 \le k \le 10$; $-25 \le l \le 25$
absorption correction	DIFABS [21 c]	empirical by ψ-scans
min./max. transmission	–	0.178/0.663
reflections collected	2992	7261
independent reflections (*z*)	2641; $R_{int} = 0.0453$	1111; $R_{int} = 0.0873$
restraints/parameters (*p*)	0/69	2/37
goodness-of-fit at F^2 (GoF)[a)]	1.099	1.197
extinction coefficient	–	0.0161(5)
abs. structure parameter	–0.03(13)	0.01(7)
largest diff. peak and hole (10^{30} e m^{-3})	1.49/–0.74	0.67/–0.42
R-indices[b)] ($I > 2\sigma(I)$)	$R1 = 0.042$; $wR2 = 0.099$	$R1 = 0.021$; $wR2 = 0.052$
R-indices[b)] (all data)	$R1 = 0.052$; $wR2 = 0.105$	$R1 = 0.022$; $wR2 = 0.052$

[a)] $GoF = \{\Sigma w(F_o^2 - F_c^2)^2/(z-p)\}^{1/2}$; [b)] $R1 = \Sigma||F_o| - |F_c||/\Sigma|F_o|$; $wR2 = \{\Sigma[w(F_o^2 - F_c^2)^2]/\Sigma[w(F_o^2)^2]\}^{1/2}$ with $w^{-1} = \sigma^2(F_o^2) + (aP)^2 + bP$ (**1**, $a = 0.0555$; $b = 2.850$; **2**, $a = 0.0054$; $b = 1.190$) and $P = (F_o^2 + 2\,F_c^2)$.

Table 2 Atomic coordinates and equivalent isotropic displacement parameters (pm^2)

The position (x; $1-x$; 1/12) of the sulfur atom S located on a twofold rotation axis is designated by the Wyckoff letter *b* [21 a]. The U_{eq} value is defined as one third of the trace of the orthogonalized U_{ij} tensor.

$(Me_2Sb)_2O$ (**1**)	$x \cdot 10^4$	$y \cdot 10^4$	$z \cdot 10^4$	$U_{eq} \cdot 10^{-1}$
Sb1	3644(1)	8676(1)	9325(1)	43(1)
Sb2	5079(1)	6550(1)	7521(1)	41(1)
O	4650(10)	8714(7)	8205(3)	47(1)
C1	5248(16)	10822(14)	9750(6)	60(2)
C2	966(14)	10020(16)	9088(6)	61(3)
C3	6795(14)	5398(13)	8448(6)	54(2)
C4	2203(15)	5629(15)	7840(8)	62(3)
$(Me_2Sb)_2S$ (**2**)	$x \cdot 10^4$	$y \cdot 10^4$	$z \cdot 10^4$	$U_{eq} \cdot 10^{-1}$
Sb	7352(1)	4906(1)	78(1)	20(1)
S	5147(1)	4853(1)	833	21(1)
C1	7247(8)	6573(8)	–660(2)	45(1)
C2	9341(7)	6801(8)	681(2)	46(1)

heavier atoms and absorption corrections, which were chosen differently for both data sets (Table 1), had been applied, the positions of the hydrogen atoms could be refined by means of a riding model and with a common isotropic displacement factor for each (**1**) or all (**2**) methyl groups. Thereafter, the final difference Fourier maps showed largest difference peaks and holes of $1.49/{-0.74} \times 10^{30}$ and $0.67/{-0.42} \times 10^{30}$ e m^{-3}, respectively. Atomic coordinates and equivalent isotropic displacement parameters of the heavier atoms are given in Table 2; bond lengths, bond angles and torsional angles are compiled in Table 3. With the exception of Fig. 6 b [21 g] all structural illustrations were prepared by means of the XP program incorporated into the SHELXTL package [21 h].

The crystallographic data – excluding structure factors – have been deposited with the Cambridge Crystallographic Data Centre, receiving the CCDC numbers 124951 (**1**) and 124952 (**2**). Copies of the data can be obtained free of charge on application to The Director, CCDC, 12 Union Road, Cambridge CB2 1EZ, UK (fax: +44 1223 336033; e-mail: deposit@ccdc.cam.ac.uk).

Results and Discussion

*Bis(dimethylstibanyl)oxane (**1**).* The x-ray structure determination of compound **1** shows the solid to be built up of bent bis(dimethylstibanyl)oxane molecules; they are arranged in zigzag chains along [010] via short intermolecular Sb··O contacts between the central oxygen atom and only one of the two dimethylstibanyl moieties (Fig. 1). This type of association gives rise to a molecular conformation that is close to *syn-anti* with torsional angles Ep1–Sb1–O–Sb2 and Ep2–Sb2–O–Sb1 of 15.7° and 177.9° (Table 3), respectively, and avoids steric hindrance between the methyl groups of neighbouring molecules. As expected from the different coordination numbers of the two dimethylstibanyl fragments, the Sb–O distances within a single molecule are not uniform. Whereas the bond not involved in the chain is found to be nearly as short as in the gaseous state (198.8(5) vs. 197.6(14) pm [11]), the other is elongated to a value of 209.9(6) pm (see below).

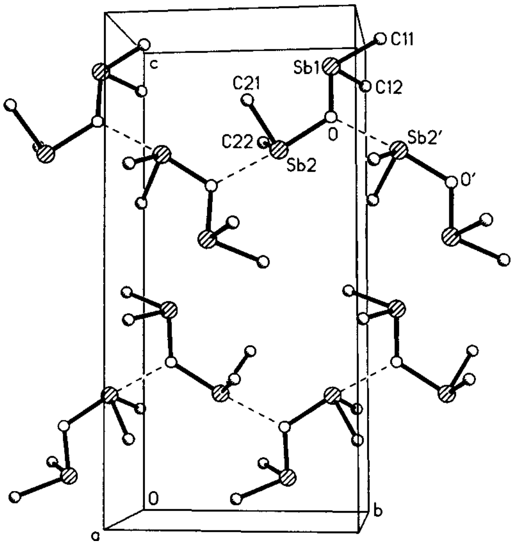

Fig. 1 Molecular model of bis(dimethylstibanyl)oxane (**1**) and the association of molecules to form zigzag chains along [010]

Weak intermolecular Sb··O interactions are indicated by thin dashed lines; primed and unprimed atoms are symmetry related by a twofold screw axis along (0.5; *y*; 0.75).

Unlike species **1** the molecules of bis(diphenylstibanyl)oxane [22] adopt the *syn-syn* conformation in the solid state so that quite obviously an analogous zigzag arrangement cannot be formed. Furthermore, when in cyclic complexes such as $([\mu_2\text{-}(H_5C_6)_2Sb\text{–}O\text{–}Sb(C_6H_5)_2]L_nM)_2$ ($L_nM = (OC)_4Cr$ [23], $(OC)_2Ni$ [24]) the antimony atoms of this compound are coordinated to transition metal carbonyl fragments, a slight but significant shortening of the mean Sb–O distance from 197.1 to 195.5 and 194.3 pm, respectively, is ascertained. Since the same observation has been reported recently for the analogous bis(dimethylstibanyl)oxane complex $([\mu_2\text{-}(Me_2Sb\text{–}O\text{–}SbMe_2)](OC)_4Cr)_2$ (198.8 to 195.3 pm [20]), we assume that the shift of electron density from antimony to the metal atom enhances the positive charge at the pnicogen atom so that in spite of its now higher coordination number the length of the *a priori* polar Sb–O bond decreases. A similar mean Sb–O bond length of 196.4 pm [25 a] was determined for the adduct $(F_2Sb)_2O \cdot 2\,(H_2N)_2C{=}O$ [25]; but in our opinion this compound is not appropriate as a comparison.

The intermolecular contact O··Sb2′, the length of which remains far below the sum of the corresponding van der Waals radii (258.5 vs. 370 pm [26 a]), and the longer bond O–Sb2 form the backbone of the infinite zigzag chain; its conformation is best characterized by a torsional angle Ep2–Sb2–O··Sb2′ of 7.9° (Table 3). In the sequence $^{1}_{\infty}$[–O(Sb)··Sb–O(Sb)··Sb] two structural features deserve special attention, namely, with an angle of 173.5° an almost complete linearity of the fragment O··Sb2′–O′ and, with an angular sum of 359.3°, the trigonal planar environment of the oxygen atom. Regarding the linearity, the atom Sb2 is located in the center of an octahedron in which two *cis*-related vertices have been removed; usually such an arrangement is referred to as ψ-trigonal bipyramidal[1] with the methyl groups and the non-bonding electron pair in equatorial and both oxygen atoms in axial positions (Fig. 2 a). The bonding situation in the O–Sb··O fragment may best be explained in terms of

---

[1] As the *s*-character of the lone electron pair at antimony is considered to be high, we make use of both possibilities to describe its coordination sphere. During the last three decades several reviews on this subject have been published [27 a, b] and detailed physical studies in this field, including antimony(III) sulfide, selenide and telluride, have been reported, for example, by *Olivier-Fourcade* and others [27 c].

Table 3 Individual bond lengths (pm), bond angles and torsional angles (deg) of bis(dimethylstibanyl)oxane (**1**) and -sulfane (**2**) from crystal structure analyses (a) and a comparison of selected x-ray diffraction (XRD) parameters with data from gas electron diffraction (GED) and density functional theory (DFT) calculations (b)

In addition to structural data the table contains symmetry operations for primed and starred atoms. Individual and mean values used for the comparison of part b) are given in italics. The symbol Ep stands for the assumed direction of the lone electron pair at antimony (see text).

a) Individual values of compounds **1** and **2**

1	O–Sb1	*198.8(5)*	Sb1–O–Sb2	*123.0(3)*	Sb1–O··Sb2′	118.5	C21–Sb2–O··Sb2′	138.3		
	O–Sb2	209.9(6)	O–Sb1–C11	97.1(3)	Sb2–O··Sb2′	117.8	C22–Sb2–O··Sb2′	–122.5		
	Sb1–C11	215.5(10)	O–Sb1–C12	96.2(3)	O··Sb2′–O′	173.5				
	Sb1–C12	214.4(10)	C11–Sb1–C12	*94.8(5)*	O··Sb2′–C21′	85.3	symmetry operation:			
	Sb2–C21	214.3(10)	O–Sb2–C21	92.3(3)	O··Sb2′–C22′	82.9	(′) ≙ (–*x* + 1; *y* + 0.5; –*z* + 1,5)			
	Sb2–C22	214.7(11)	O–Sb2–C22	91.5(3)	Sb2–O–Sb1–C11	148.0				
	O··Sb2′	258.5	C21–Sb2–C22	99.4(5)	Sb1–O–Sb2–C21	–51.7	characteristic mean values:			
					Sb2–O–Sb1–C12	–116.7	Sb–C	*214.7*	O–Sb2–C	91.9
					Sb1–O–Sb2–C22	47.5	O–Sb1–C	*96.7*	O··Sb2′–C	84.1
2	S–Sb	*249.8(1)*	Sb–S–Sb′	*92.35(5)*	S*··Sb–C1	85.6	symmetry operations:			
	Sb–C1	214.5(5)	S–Sb–C1	94.2(2)	S*··Sb–C2	83.7	(*) ≙ (*x* – *y* + 1; *x*; *z* – 0.166);			
	Sb–C2	215.1(5)	S–Sb–C2	93.2(1)	S–Sb··S*	176.8	(′) ≙ (–*y* + 1; –*x* + 1; –*z* + 0.166);			
	Sb··S*	316.4	C1–Sb–C2	*95.9(3)*	Sb–S··Sb″	109.9	(″) ≙ (*x* – *y*; –*y* + 1; –*z*);			
					Sb–S··Sb‴	134.0	(‴) ≙ (*y*; –*x* + *y* + 1; *z* + 0.166)			
	characteristic mean values:				Sb″··S··Sb‴	83.4				
	Sb–C	*214.8*	S–Sb–C	*93.7*	Sb′–S–Sb–C1	173.5	Sb′–S–Sb–C2	–90.5		

b) Selected x-ray diffraction parameters in comparison with data from GED and DFT

	1 (E = O) XRD	GED [11]	DFT [11]	**2** (E = S) XRD	GED [12]	DFT [11]
E–Sb	*198.8(5)*	197.6(14)	204.3	*249.8(1)*	241.4(4)	248.9
Sb–C (mean)	*214.7*	214.4(9)	219.4	*214.8*	213.2(3)	220.0
E–Sb–C (mean)	*96.7*	92.3(6)	95.2	*93.7*	92.6(6)	94.6
C–Sb–C	*94.8(5)*	97.8(18)	93.5	*95.9(3)*	95(3)	94.0
Sb–E–Sb	*123.0(3)*	122.3(16) (*syn-syn*) 131.1(18) (*syn-anti*)	119.0 (*syn-syn*) 127.7 (*syn-anti*)	*92.35(5)*	98.7(5) (*syn-syn*) 104.5(5) (*syn-anti*)	101.4 (*syn-syn*) 107.4 (*syn-anti*)
Ep1–Sb1–O–Sb2	15.7	±28(4) (*syn-syn*)	±18.6 (*syn-syn*)	–	–	–
Ep2–Sb2–O–Sb1	177.9	[0; 180] (*syn-anti*)	0; 180 (*syn-anti*)	–	–	–
Ep–Sb–S–Sb′	–	–	–	41.5	±33(4) (*syn-syn*) [0; 180] (*syn-anti*)	0.0 (*syn-syn*) 0; 180 (*syn-anti*)

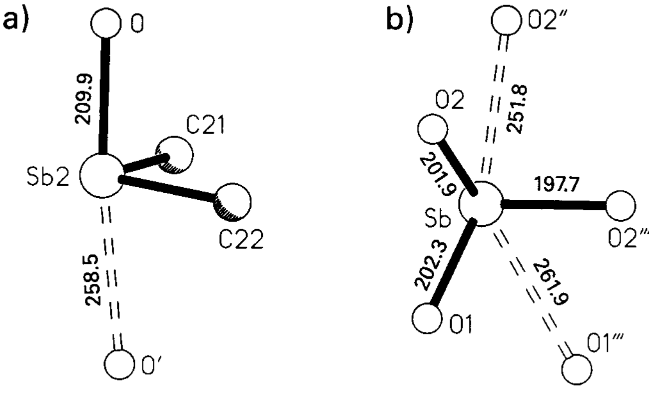

Fig. 2 Different coordination spheres of the antimony atoms in the solid-state structures of bis(dimethylstibanyl)oxane (**1**) and valentinite

The figure shows (a) an octahedron with two *cis*-related vertices removed (*ψ*-trigonal bipyramid) and (b) a square pyramid (*ψ*-octahedron). Dashed open lines indicate weak Sb··O interactions. Except for the symmetry-related atom O1‴ (*x*; 0.5 – *y*; 0.5 + *z*) the labeling of atoms has been adopted from Table 3 and publication [3b], respectively.

a strongly asymmetric four-electron three-center bond utilizing the $\sigma_{\text{Sb–O}}$ and $\sigma^*_{\text{Sb–O}}$ orbitals. As for the environment at oxygen the bond angle Sb1–O–Sb2 is found to be slightly smaller than the corresponding parameter determined or calculated for the gaseous molecule in its *syn-anti* conformation (123.0(3)° vs. 131.1(18)° or 127.7°; Table 3). Furthermore, the solid state structure of compound **1**, though characterized by three different Sb–O distances, anticipates the completely symmetric situation realized in the star-shaped cation of tris(dimethylstibanyl) oxonium bromide (Sb–O 211.6(1) pm), which has been isolated and characterized by some of us a few years ago [28].

Comparison with Valentinite. The intermolecular interactions in solid bis(dimethylstibanyl)oxane (**1**) have to be ascribed to the field of secondary bonding ([29, 30]; see also [31]) – a phenomenon which is observed frequently with antimony compounds. In order to allow a reasonable interpretation of the special features discussed above, we inspected the known structure of valentinite (Antimonblüte, Weißspießglanz) [3], the orthorhombic modification of antimony(III) oxide, for similarities. As can be seen in Fig. 3, the mineral is built up of infinite Sb–O double chains

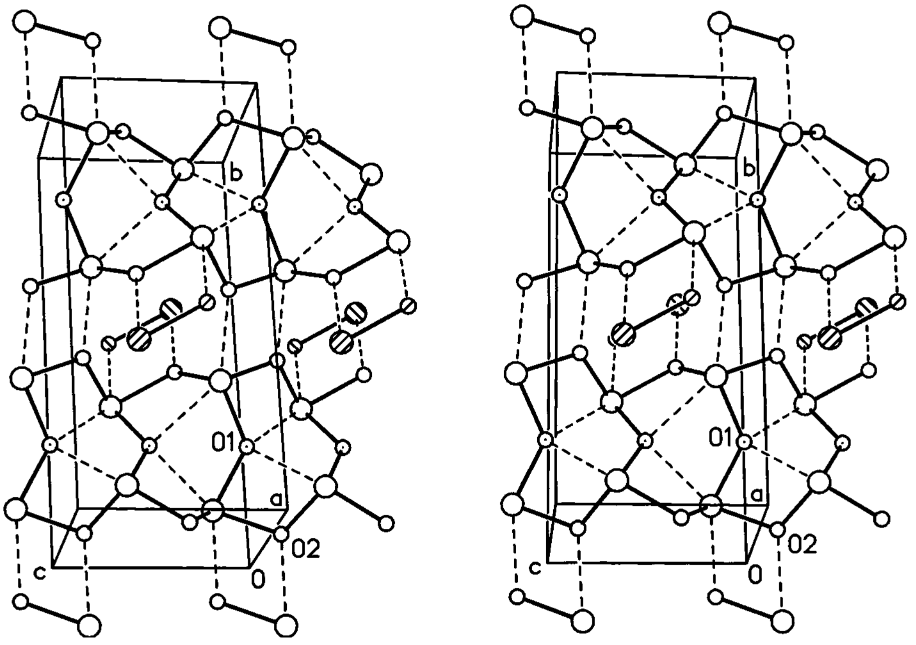

Fig. 3 Stereoscopic view of oxygen-bridged Sb–O double chains aligned along [001] in the structure of valentinite, the orthorhombic modification of antimony(III) oxide

The figure is based on atomic coordinates given in the literature [3b]. Antimony and oxygen atoms are represented by large and small circles, respectively; solid lines stand for Sb–O bonds, thin dashed ones for weak Sb··O interactions (see Fig. 2b). To illustrate the linkage between different layers, four translationally identical Sb–O units, two of an upper- (⊘) and two of a lower-lying double chain (⦸), are additionally shown.

along [001], the opposing antimony atoms of which are bridged by oxygen in such a way that strongly puckered eight-membered rings are formed. Considering the three different bond lengths between antimony (Sb) and the two crystallographically independent oxygen atoms O1 and O2 in the bridge (O1–Sb 202.3(4) pm) and in the single chain (O2–Sb 201.9(6), O2‴–Sb 197.7(7) pm [3b]; Fig. 2b), respectively, one finds only two to deviate significantly, by about 8 and 3 pm, from the distances O–Sb2 of 209.9(6) and O–Sb1 of 198.8(5) pm in compound **1** (Table 3); the third one matches almost exactly the length of the shorter bond O–Sb1 and coincides with the value of 197.7(1) [2c] reported for senarmontite [2], the cubic modification of antimony(III) oxide.

In the crystal structure of valentinite two types of secondary Sb··O contacts are observed. Within the aforementioned double chains the bridging oxygen atom O1 is involved in two contacts of equal length increasing its coordination number to (2 + 2). A second type of Sb··O contact is incorporated in centrosymmetric four-membered Sb··O–Sb··O rings between the double chains (Fig. 3); it connects the five-coordinate antimony atom in a *strongly* distorted square pyramidal (ψ-octahedral) environment (Fig. 2b; angles between 67.0° and 149.1°) with the trigonal-planar coordinate oxygen atom O2. In a manner similar to compound **1**, its angles sum up to 357.3°; here, however, with values of only 149.1° and 139.2° at antimony the sequences O1–Sb··O2″ and O2–Sb··O1‴ deviate considerably from linearity. Nevertheless, the different Sb··O contact distances within (261.9 pm) and between the double chains (251.8 pm) both approach closely the related value (258.5 pm) of bis(dimethylstibanyl)oxane (**1**).

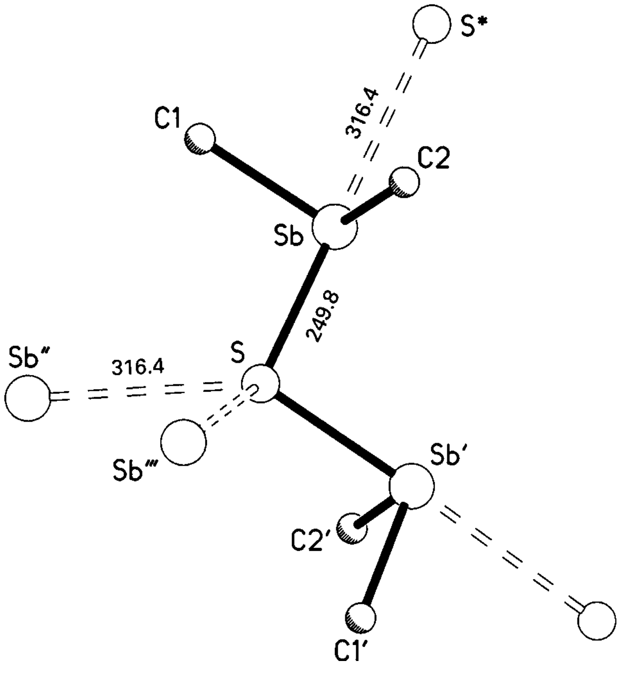

Fig. 4 Molecular model of bis(dimethylstibanyl)sulfane (**2**) and its relationship to antimony and sulfur atoms of adjacent species

The weak Sb··S interactions are indicated by dashed open lines; the positions of symmetry related atoms may be obtained from the values of Table 2 by operations given in Table 3.

Bis(dimethylstibanyl)sulfane (2). As can be taken from Fig. 4, the molecules of compound **2** differ from those of bis(dimethylstibanyl)oxane (**1**) not only by an almost *syn-syn* conformation exhibiting symmetry-related torsional angles Ep–Sb–S–Sb′ and Ep′–Sb′–S–Sb of 41.5° (Table 3), but also by a totally different packing and an increase in coordination numbers. They change from (2 + 1) for oxygen to (2 + 2) for sulfur; furthermore, the antimony atom of every dimethylstibanyl group is now linked to *two* chalcogen atoms. As a consequence, instead of a one-dimensional chain in the oxygen derivative **1** a three-dimensional network is formed (see below).

With the two sulfur atoms S and S* in axial and the carbon atoms C1 and C2 of two methyl groups as well as the non-bonding electron pair in equatorial sites, the coordination sphere at antimony is again described as an octahedron with two *cis*-related vertices removed or as a ψ-trigonal bipyramid. At 249.8(1) pm the length of the two symmetry-related S–Sb bonds slightly exceeds the Schomaker-Stevenson corrected sum of covalent radii (244 pm [26 c]) and to a greater extent the value of 241.4(4) pm already determined by electron diffraction for the gaseous molecule [12]. In our opinion this elongation has to be correlated with the higher coordination number of sulfur in the solid (see below). For comparison, in the compounds $(H_5C_6)_2Sb\text{–}S\text{–}Sb(C_6H_5)_2 \rightarrow Cr(CO)_5$ [23] and $[MeSb(\text{–}S\text{–}SbMe_2)_2](OC)_4Cr$ [20] the uncomplexed parts of the two stibanylsulfane ligands show S–Sb distances of 244.6(1) and 243.3(1) pm, whereas coordination of the antimony atoms is accompanied by a shortening of the adjacent S–Sb bonds to values of 240.2(1) and 241.2(1) pm, respectively. Since similar bond lengths of 242.1(2) and 242.4(2) pm have been reported recently by some of us [20] for the cyclic complex $[\mu_2\text{-}(Me_2Sb\text{–}S\text{–}SbMe_2)(OC)_4Cr]_2$, we are convinced that the interpretation of this shortening already given above for the related oxygen compounds holds for the stibanylsulfane complexes as well. In contrast, polymeric dimethylstibanyl(dimethylthiophosphoranyl)sulfane [32] exhibits a much longer distance of 255.5(2) pm.

The formal replacement of oxygen for sulfur is accompanied by a drastic change of the corresponding bond angle from 123.0(3)° in compound **1** to 92.35(5)° in compound **2** (Table 3). Similarly, for the gaseous molecules with *syn-syn* conformation Sb–O–Sb and Sb–S–Sb angles of 122.3(16)° and 98.7(5)°, respectively, were determined by electron diffraction. This decrease of the central angle is a phenomenon generally observed when in congenerous compounds a pnicogen or chalcogen atom of either the second or the third period is bound to two less electronegative elements. In the compounds discussed here, the differences in bond angles of 30.7° and mean bond lengths of 45.5 pm balance each other to such an extent that both the intramolecular Sb··Sb contacts adopt equal lengths of 359.2 and 359.3 pm; these values are considerably below twice the van der Waals radius of antimony (440 pm [26 a]).

As for the intermolecular Sb··S contacts, which are responsible for the unique molecular arrangement of compound **2**, the pertinent angles Sb··S··Sb and Sb–S··Sb range from 83.4° to 134.0°; together with the angle Sb–S–Sb′ already discussed above they define a strongly distorted tetrahedron at sulfur. Quite obviously the extreme variation of these values is to a great extent brought about by the molecular packing (see below). At 316.4 pm the two symmetry-related secondary Sb··S bonds [29, 30] are found again to be by far shorter than the corresponding sum of van der Waals radii (400 pm [26 a]). Since in our opinion the high affinity of antimony for sulfur is evidently demonstrated by the formation of an 1 : 1 adduct[2)] between *cyclo*-octasulfur and antimony(III) chloride [33], its Sb··S distances were supposed to be appropriate for a comparison; however, at 333 and 349 pm they are rather long with respect to bis(dimethylstibanyl)sulfane (**2**). Furthermore, for the following complexes of cyclic thioethers which were selected from a larger number of compounds the values given in parentheses have been reported:
1,3,5-trithia-*cyclo*-hexane · $SbCl_3$ (326 pm) [35 a],
1,4-dithia-*cyclo*-heptane · $SbCl_3$ (313 to 340 pm) [35b],
1,4,7-trithia-*cyclo*-nonane · $SbCl_3$ (316 to 341 pm) and
1,4,7,10,13,16-hexathia-*cyclo*-octadecane · 2 $SbCl_3$ (297 to 346 pm) [36].

The Sb–C bond lengths of compounds (**1**) and (**2**), although associated with relatively high standard deviations, vary only slightly from 214.3(10) to 215.5(10) pm and 214.5(5) to 215.1(5) pm, respectively (Table 3); the mean corresponds fairly well to the sum of covalent radii (218 pm [26 a]). As far as the bond angles at antimony are concerned, only in the oxygen derivative **1**, which is characterized by two different dimethylstibanyl groups, a small but significant effect of intermolecular association can be recognized. Whereas at the antimony atom Sb1, which is not involved in secondary bonding (Fig. 1), the angles C–Sb–C and O–Sb–C are found to be quite uniform (94.8(5)° to 97.1(3)°), the corresponding values of the second group vary from 91.5(3)° or 92.3(3)° to 99.4(5)°; in our opinion the increase of the angle C21–Sb2–C22 is caused by the relatively short O′··Sb2 contact of 258.5 pm. As a result of the by far longer Sb··S contacts (316.4 pm), in compound **2** all bond angles at antimony lie in a narrow range of 93.2(1)° to 95.9(3)°.

Salient features in the crystal structure of compound **2** (Fig. 5) are double helices generated by 6_5 screw axes along [001] and built up of alternating short S–Sb bonds (249.8(1) pm) and longer Sb··S* contacts (316.4 pm); remarkably, there is no *direct* connection between the individual chains. As they are symmetry-related by twofold rotation axes in, for example, (2*x* – 1; *x*; 5/12), both helices are left-handed but display a phase shift of *c*/2 and, with respect to the 6_5 screw

---

[2)] As the structure of the adduct $SbI_3 \cdot 3\,S_8$ [34] is governed by intermolecular S··I and Sb··I interactions, this compound should not be chosen for a comparison.

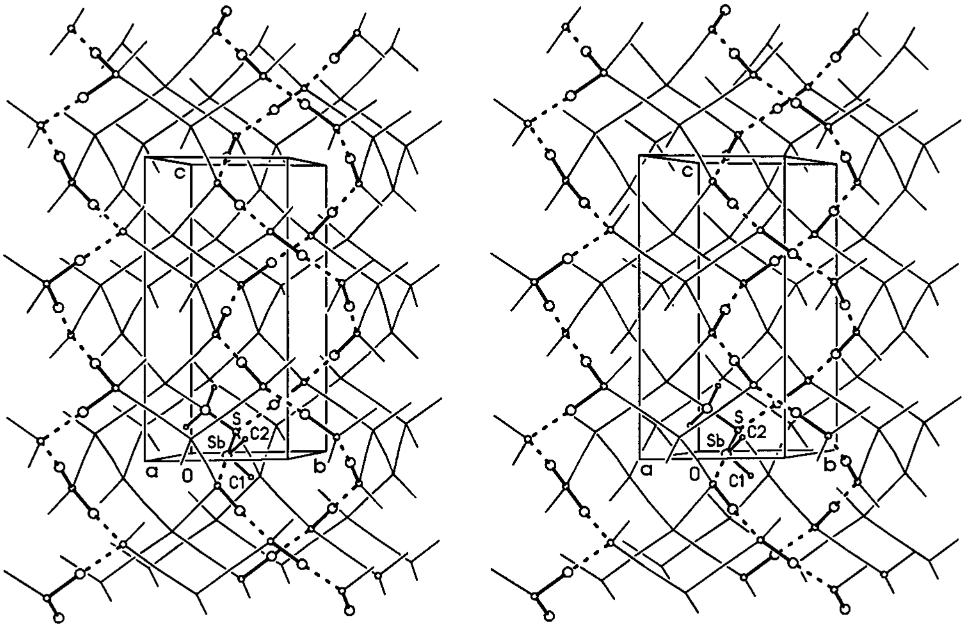

Fig. 5 Crystal structure of bis(dimethylstibanyl)sulfane (**2**) in stereoscopic view

To illustrate the topological relationships as clearly as possible, a simple wire model has been applied, but for three single helices, which are discussed at some length in the text, the sulfur and antimony atoms, the S–Sb bonds and the Sb··S contacts are highlighted as small and large circles, thick solid lines (sticks) and solid dashed lines, respectively. Carbon atoms are not shown, with the exception of the molecule referring to the asymmetric unit (Table 2).

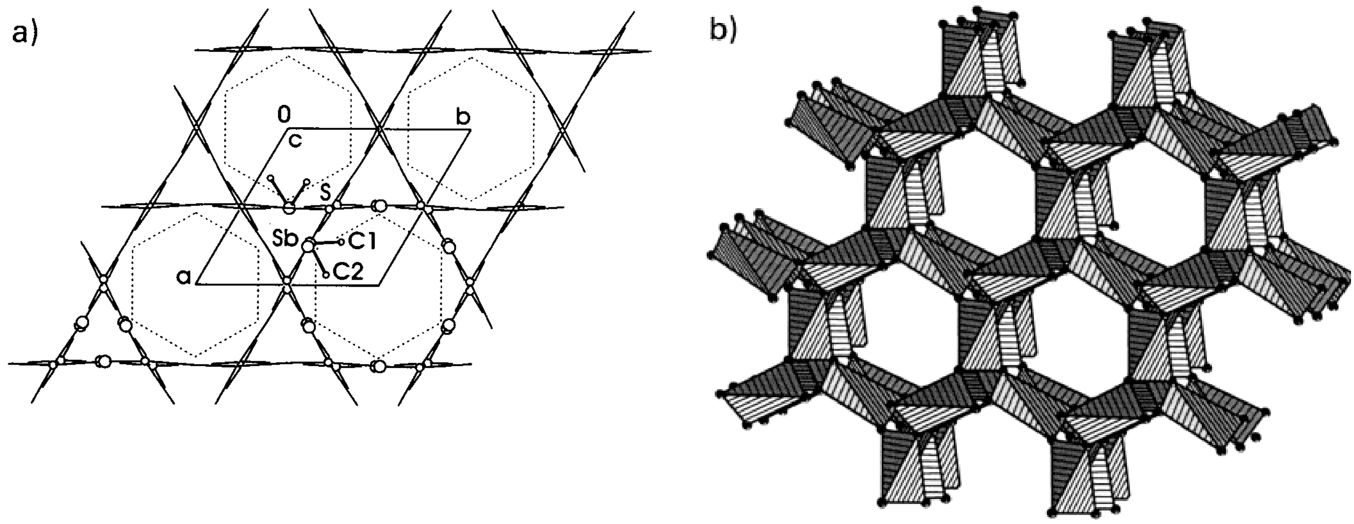

Fig. 6 Crystal structure of bis(dimethylstibanyl)sulfane (**2**) viewed along [001]

a) Parallel projection based on Fig. 5. One should note that only hexagons formed by the antimony atoms (large circles) give rise to a honeycomb-like pattern.

b) Simplified representation generated with the program DIAMOND [21 g]. The illustration shows only vertex-sharing SSb$_4$ tetrahedra; the hexagonal channels contain the methyl groups (see text).

axes, a reverse sequence of S–Sb bond and Sb··S contact. Since, with an angle of 176.8° at the antimony atom of the (1 + 1)-coordinate dimethylstibanyl group, the array S–Sb··S* does not deviate significantly from linearity, the rather large Sb–S··Sb‴ value of 134.0° at the (2 + 2)-coordinate sulfur atom is almost exclusively responsible for the kink within a helix. Therefore, its pitch can be described by a torsional angle of –36,4° between four successive sulfur atoms and the cross-section of the double helices approximates a regular hexagon.

Indeed, hexagonal tubes as spanned, for example, by the antimony atoms (Fig. 6 a) and their honeycomb-like pattern (Fig. 6 b) become particularly obvious when the crystal structure is viewed along the 6_5 screw axes. In the latter representation the heavy-atom framework is depicted as an arrangement of distorted vertex-sharing SSb$_4$ tetrahedra with the sulfur atoms hidden at the centers. The methyl groups are located inside these hexagonal tubes (Fig. 6 a), but owing to the twofold rotation axes the two sets of a molecule are found in different interiors. In this context one should point out that such a structural separation of the more inorganic and the more organic parts of a molecule has frequently been observed with organoelement compounds.

In an *individual* 6_5 helix, each bis(dimethylstibanyl)sulfane molecule contributes only one antimony atom to its backbone, whereas the remaining dimethylstibanyl groups point outwards (Fig. 5). Since, however, the two halves of a single molecule are symmetry-related by a twofold rotation axis, each double helix is connected with a total of six adjacent ones by sharing the sulfur atoms that are arranged at the axial edges of the hexagonal prisms (Fig. 6 a). As a consequence, the cross-linking of double helices gives rise to different helices with a trigonal projection (Fig. 6 a); they are right-handed though coiling around 3_2 screw axes (Fig. 5). This apparent contradiction is readily resolved when the inherent symmetry of such a helix is carefully inspected. Indeed, owing to the sequence $^1_\infty[\mathrm{Sb{-}S{-}Sb}\cdot\cdot\mathrm{S}\cdot\cdot]$, in which a pair of S–Sb bonds is followed by a pair of Sb··S contacts each, the 3_2 screw axis by itself correlates only every *second* sulfur atom so that the resulting conjunction line – though chemically meaningless – describes a left-handed helix. Finally, the two subsets of sulfur atoms are symmetry-related by 2_1 screw axes perpendicular to [001]. Within the three-dimensional net thus formed, strongly puckered twelve-membered macrocycles with the sequence $[\mathrm{Sb{-}S{-}Sb}\cdot\cdot\mathrm{S}\cdot\cdot\mathrm{Sb{-}S}\cdot\cdot]_2$ can be identified as shortest circuits.

From a topological point of view the arrangement of sulfur and antimony atoms in compound **2** is identical to that of silicon and oxygen in the high temperature modification of quartz (β-quartz) [37]. Since, however, the silicon atoms in this structure occupy positions of site symmetry 222 and all Si–O bonds are of equal length, translational identity is already achieved after one turn (360°) of the trigonal single helices and after half a turn (180°) of the hexagonal double helices (cf. Fig. 5). In terms of symmetry, $P6_422$, the space group of β-quartz, constitutes a minimal *klassengleiche* supergroup of index 2 in relation to $P6_522$, the space group of bis(dimethylstibanyl)sulfane (**2**), the group-supergroup transition being associated with a bisection of the lattice parameter *c* and a transformation of the left-handed 3_2 screw axes in space group $P6_522$ into its right-handed counterpart 3_1 in $P6_422$. As already derived from the symbol of the achiral space group $P6_3/mmc$, the structural relationships between β-tridymite [38] and compound **2** are by far less, and we have therefore not attempted a detailed analysis.

Some Remarks on the Space-Group of Compound ***2***. Following an inspection of crystallographic databases [39], the enantiomorphous space groups $P6_122$ and $P6_522$ appear more frequently than originally supposed. In the field of organic and organoelement compounds, including metal complexes mostly with large organic ligands, approximately fifty structures were reported. The compilation includes references to the well-known high-temperature modifications of alkane/urea inclusion compounds such as the 1,10-dibromodecane or 1,12-dibromododecane derivative [40], optically active dilactylamide, the molecules of which are arranged in infinite chains by hydrogen bonds [41], or even bis(η^5-*cyclo*-pentadienyl)bis(η^1-*cyclo*-pentadienyl)titanium, the structure of which does not show any discernible intermolecular interactions [42]. With respect to the much smaller number of inorganic representatives, the oft studied complex $\mathrm{Cs[CuCl_3]}$ [43] and the isostructural fluorides $\mathrm{AuF_3}$ [44] and $\mathrm{AgF_3}$ [45] have to be mentioned first; their helical chains are built up by strongly distorted face-sharing octahedra of chloride anions surrounding the $\mathrm{Cu^{2+}}$ cations [43 b] and of planar, only slightly distorted squares joined by a symmetrical sharing of two *cis*-related fluoride ligands, respectively. Furthermore, the inclusion compound $\mathrm{Sn[Ta_2Cl_9]_2 \cdot C_6H_6}$ isolated from the reduction of tantalum(V) chloride with tri-*n*-butylstannane also belongs to this group; in the rather complicated structure the $\mathrm{[Ta_2Cl_9]^-}$ anions are arranged in chains coiling around the 6_5-screw axis [46].

However, to our knowledge the borophosphates $\mathrm{M^I(H_2O)_2M^{II}[BP_2O_8] \cdot H_2O}$ are the only class of inorganic compounds with vertex-sharing $\mathrm{EO_4}$ tetrahedra (E = B, P), for which space group $P6_122$ has been reported so far [47]. Their framework $^1_\infty\{(\mathrm{M^I[BP_2O_8]})^{2-}\}$ features double helices which are built up of $\mathrm{M^I}$ cations on the one hand and of alternating $\mathrm{BO_4}$ and $\mathrm{PO_4}$ moieties on the other. Since the channels formed are filled with water molecules, the structures of the borophosphates show a relatively high degree of similarity to that of bis(dimethylstibanyl)sulfane (**2**), the channels of which contain the methyl groups.

Comparison with Stibnite. As reflected by the German mineral name "Grauspießglanz" (*Spieß* means *spear*), the structure of stibnite [4] features $^1_\infty[\mathrm{Sb_4S_6}]$ ribbons aligned along [010] (Fig. 7). If, as a first approximation, all direct Sb–S bonds and contacts *within* these entities (Fig. 8 a) are taken as topologically equivalent, the ribbons may be described as zigzag chains of face-sharing $\mathrm{Sb_4S_4}$-cubes, the outer antimony atoms of which are bridged in pairs by additional sulfur atoms. In other words, the ribbons are regarded as sections of the rock salt (halite) structure (Fig. 8 b). This view is

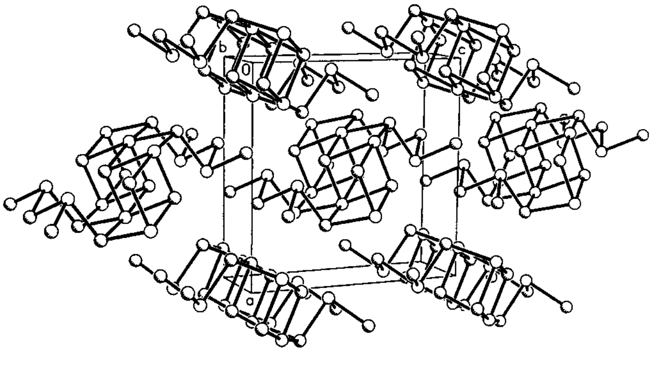

Fig. 7 Almost hexagonal close packing of $^1_\infty[\mathrm{Sb_4S_6}]$ ribbons in the crystal structure of stibnite (space group *Pnma*)

In contrast to the following more detailed representation of Figure 8 c no distinction between primary and *short* secondary (coordinative) Sb–S bonds is made and in addition distances exceeding 285.4 pm are not shown.

for example justified by the observation that sodium dithioantimonate(III) ($NaSbS_2$) [48] adopts an ordered variant of that structural type.

If in contrast to this generalized approach the weak Sb··S contacts within the ribbons are totally ignored, the rather complicated framework may be described alternatively by two sequences of Sb_2S_2 quadrangles, the common vertices of which are occupied by the antimony atoms Sb2 (Fig. 8a). Owing to a center of inversion in (0.5; 0.5; 0.5) the sequences are found to be shifted relative to each other so that short bonds of 245.6 pm between the antimony atoms Sb2 of one layer and the so-called inner sulfur atoms S2 of the second layer become possible. The arrangement depicted so far is completed by two Sb1–S1 zigzag chains which are connected to the outer sulfur atoms of each sequence by nearly perpendicular Sb1–S3 bonds. Remarkably, the structural feature of vertex-sharing quadrangles with square pyramidally (ψ-octahedrally) coordinate antimony atoms is observed for example in the polymeric ${}^{1}_{\infty}[Sb_2S_5{}^{4-}]$ anions of the thioantimonate(III) $Sr_3Sb_4S_9$ ([49]; see also [50], p. 267).

When the structures of stibnite and rock salt (Fig. 8) are compared to each other in detail with respect to the individual S–Sb distances as listed in Table 4, considerable deviations from an idealized arrangement become obvious. Indeed, significant distortions are expected since the Allred-Rochow electronegativities [26b] of antimony (1.82) and sulfur (2.44) differ by only 0.62 units and the bonding situation has therefore to be considered as mostly covalent[3]. As a consequence, the antimony and sulfur atoms are *a priori* expected to be found three- and two-coordinate in a trigonal pyramidal and bent arrangement, respectively, but only in case of the outer antimony (Sb1) and the bridging sulfur atom S1 (Fig. 8a) an unambiguous assignment of *three* or *two* primary bonds is possible (Table 4). However, any attempt to assign localized two-center two-electron bonds in the tetragonal pyramidal (ψ-octahedral)[4] coordination sphere of Sb2 (c. n. = 1 + 2 + 2) and the approximately trigonal pyramidal environments of S2 and S3 (c. n. = 1 + 2) would require an *arbitrary* discrimination between primary and *short* secondary (coordinative) bonds. Despite these restrictions, however, for didactic reasons such a representation of the stibnite structure has been incorporated in Fig. 8.

In order to classify the different distances, we carried out a bond-valence analysis (Table 4) making use of *I. D. Brown's* relationship [52]. Surprisingly, the original standard value R_0 for S–Sb^{III} and S–Sb^{V} bonds of 245 pm afforded valence sums dif-

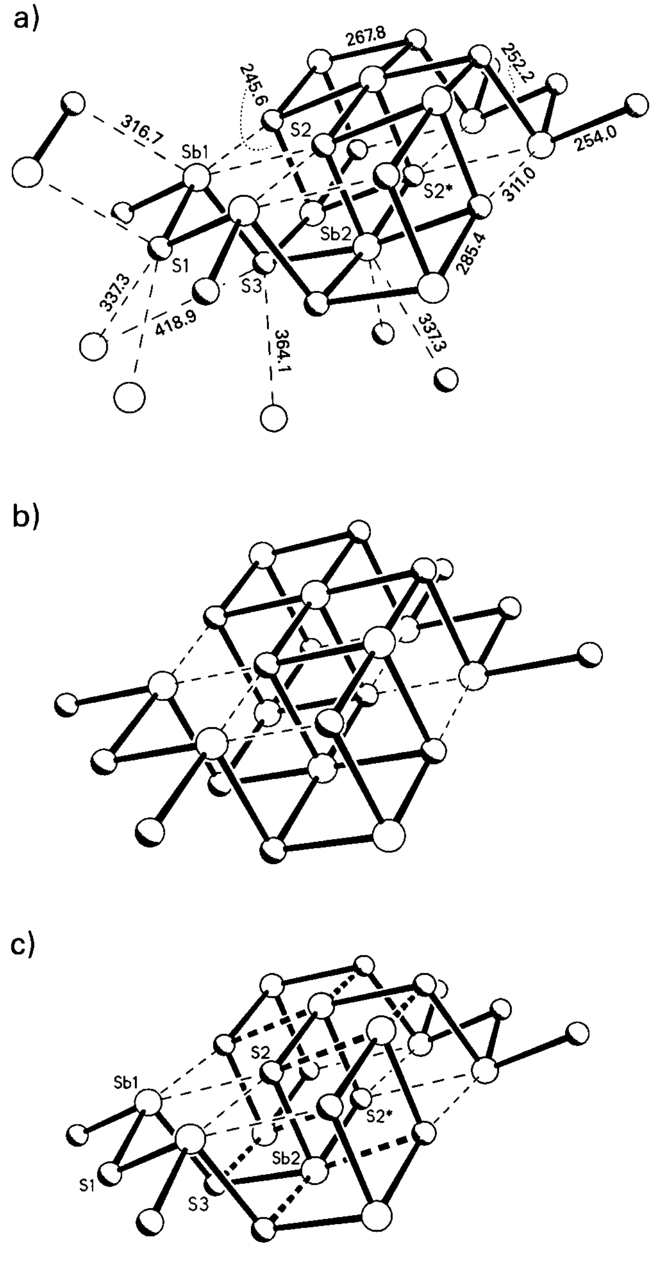

Fig. 8 Relationships between the stibnite and the rock salt structure

a) Centrosymmetric section of a ${}^{1}_{\infty}[Sb_4S_6]$ ribbon aligned along [010] as shown in Fig. 7 at the center of the unit cell. S–Sb bonds up to a length of 285.4 pm and contacts in a range from 311.0 to 418.9 pm are depicted as solid and thin dashed lines, respectively. For the coordinates of labeled atoms see Table 4.

b) Corresponding section of an undistorted rock salt structure. The representation of interatomic distances within a ribbon follows part a).

c) Structure of stibnite from a covalent but more traditional point of view. In order to distinguish *arbitrarily* between primary and *short* secondary (coordinative) S–Sb bonds, solid and dashed solid lines have been employed. Thin dashed lines indicate longer Sb··S contacts between atoms of the same ribbon.

---

[3] One has to point out that in this approach structural relationships to metal sulfides of the same stoichiometry such as U_2S_3 ([51]; see also [15]) and electronic interactions, which can be classified as mostly ionic, are deliberately neglected.

[4] At this level of discussion weak Sb··S contacts between different ribbons are not taken into consideration.

Table 4 Bond-valence analysis of the stibnite structure

Individual bond-valences s_i (valence units, v. u.) were calculated for all heteronuclear ligands L_i at distances R_i up to 450 pm making use of *I. D. Brown's* formula $s_i = (R_i/R_0)^{-N}$ [52] and the parameters ($R_0 = 241.6$ pm; $N = 6$); in addition, the sum of bond-valences is specified for each central atom Z. To obtain a coherent set of atoms, we transformed the published coordinates [4 c] and changed the numbering scheme accordingly; for clarity, ligands of adjacent ribbons were placed in parentheses. One should note that *Wang* and *Liebau* [27 b] have reported a brief bond- valence analysis of stibnite applying, however, a modified approach.

Z	L_i	Coordinates and symmetry operations	R_i	s_i (v. u.)
Sb1		0.5293; 0.75; 0.1739		$\sum^{i} s_i = 3.0$
	S3	x; y; z	252.2	0.77
	S1	x; y; z	254.0	0.74
	S1	x; $y + 1$; z	254.0	0.74
	S2	x; y; z	311.0	0.22
	S2	x; $y + 1$; z	311.0	0.22
	(S1)	$-x + 1$; $-y + 1$; $-z$	316.7	0.20
	(S3)	$x - 0.5$; y; $-z + 0.5$	364.1	0.09
S1		0.6251; 0.25; 0.0614		$\sum^{i} s_i = 1.9$
	Sb1	x; y; z	254.0	0.74
	Sb1	x; $y - 1$; z	254.0	0.74
	(Sb1)	$-x + 1$; $-y + 1$; $-z$	316.7	0.20
	(Sb2)	$-x + 1.5$; $-y$; $z - 0.5$	337.3	0.14
	(Sb2)	$-x + 1.5$; $-y + 1$; $z - 0.5$	337.3	0.14
S3		0.7079; 0.75; 0.3083		$\sum^{i} s_i = 2.0$
	Sb1	x; y; z	252.2	0.77
	Sb2	x; y; z	267.8	0.54
	Sb2	x; $y + 1$; z	267.8	0.54
	(Sb1)	$x + 0.5$; y; $-z + 0.5$	364.1	0.09
	(Sb2)	$-x + 1.5$; $-y + 1$; $z - 0.5$	418.9	0.04
Sb2		0.6495; 0.25; 0.4640		$\sum^{i} s_i = 3.0$
	S2	x; y; z	245.6	0.91
	S3	x; y; z	267.8	0.54
	S3	x; $y - 1$; z	267.8	0.54
	S2	$-x + 1$; $-y$; $-z + 1$	285.4	0.37
	S2[a]	$-x + 1$; $-y + 1$; $-z + 1$	285.4	0.37
	(S1)	$-x + 1.5$; $-y$; $z + 0.5$	337.3	0.14
	(S1)	$-x + 1.5$; $-y + 1$; $z + 0.5$	337.3	0.14
	(S3)	$-x + 1.5$; $-y + 1$; $z + 0.5$	418.9	0.04
S2		0.4503; 0.25; 0.3769		$\sum^{i} s_i = 2.1$
	Sb2	x; y; z	245.6	0.91
	Sb2	$-x + 1$; $-y$; $-z + 1$	285.4	0.37
	Sb2	$-x + 1$; $-y + 1$; $-z + 1$	285.4	0.37
	Sb1	x; y; z	311.0	0.22
	Sb1	x; $y - 1$; z	311.0	0.22

[a] This atom is marked with an asterisk in Figure 8.

fering considerably from the expected results of 3.0 and 2.0 valence units (v. u.) for antimony and sulfur. Therefore a slightly shorter distance R_0, which at 241.6 pm is very close to the length of the S–Sb^{III} single bond (241.4(4) pm) in gaseous bis(dimethylstibanyl)sulfane (**2**) [12], was applied; remarkably, a similar approach has been reported by *Skowron* and *Brown* [53] for a series of lead thioantimonates(III). With S · · Sb distances up to a limit of 420 pm taken into account, our calculations resulted in coinciding sums of 3.0 v. u. for both antimony atoms, indicating the valences of these atoms to be completely balanced – despite of quite different coordination numbers of (3 + 3 + 1) and (1 + 2 + 2 + 2 + 1) for Sb1 and Sb2, respectively.

As with numerous chalcogenoantimonates(III) [50], an adequate explanation of the bonding situation in stibnite is based on the finding that the valences of *trans*-related bonds in the distorted octahedral and tetragonal pyramidal (ψ-octahedral)[4)] coordination spheres of the antimony atoms Sb1 and Sb2 (Fig. 8 a) add to 1.0 and 0.9 v. u., respectively. According to that, in these almost linear fragments the bonding may be qualitatively described in terms of three-center four-electron bonds with a differing degree of asymmetry (Sb1, 252.2 vs. 316.7 pm, 254.0 vs. 311.0 pm; Sb2, 267.8 vs. 285.4 pm). In this context, one has to point out that more than thirty years ago *H. Krebs* used similar but not the same arguments of mesomeric *pσ* bonds in his famous textbook on the fundamentals of inorganic crystal chemistry [15]. At present, the discussion of related Cl–Sb · · Cl systems should also be taken into account [30].

With distances of 245.6, 252.2 and 254.0 pm for Sb2–S2, Sb1–S3 and Sb1–S1, respectively, the three shortest bond lengths of the mineral stibnite are found in the same range as the corresponding value of 249.8(1) pm (Table 3 a) determined for solid bis(dimethylstibanyl)sulfane (**2**). Since in *trans* position to these bonds only weak Sb · · S interactions can be observed, these four values are only *slightly* influenced by a participation in three-center four-electron bonds. However, from the corresponding valences in stibnite (0.91, 0.77 and 0.74 v. u.; Table 4) and bis(dimethylstibanyl)sulfane (**2**, 0.82 v. u.) as well as from a comparison with the S–Sb bond length of only 241.4(4) pm for compound **2** in the gaseous state (Table 3 b; [12]), a relatively small but nevertheless significant influence of weak Sb · · S interactions and hence of higher coordination numbers in the solids becomes evident. In conformity with these findings the contact of 311.0 pm (0.22 v. u.), which occurs between the atoms Sb1 and

S2 of the same ribbon[5], and higher values of 316.7 and 337.3 pm (0.20 and 0.14 v. u.) between adjacent ribbons of stibnite correspond very well with a length of 316.4 pm (0.20 v. u.) determined for the two secondary Sb··S bonds of compound **2** by x-ray analysis. As a consequence a sum of 1.02 v. u. is achieved even for the organoelement species.

Preparative Section

All operations were carried out under an argon atmosphere with strict exclusion of air.

Bis(dimethylstibanyl)oxane (**1**). 21.62 g (93.30 mmol) of bromodimethylstibane were added dropwise to a stirred solution of sodium hydroxide (3.92 g, 98.01 mmol) in 15 ml of water. After two hours of further stirring at ambient temperature the product was separated and the aqueous phase was extracted with three portions of 40 ml of petroleum ether. Product and organic solution were combined and dried with anhydrous sodium sulfate; after removal of the solvent at a pressure of 80 mbar, distillation of the remaining liquid at 57.5 to 58.5 °C/7 mbar furnished compound **1** with 98.5% purity. 59.7% yield (8.9 g, 27.8 mmol).

Characterization: colorless, malodorous liquid.

NMR (benzene-d_6 solution). ^{1}H (200 MHz): 0.84 ppm (s, $^1J_{CH}$ = 131.2 Hz, CH_3); ^{13}C{^{1}H} (50 MHz): 13.31 ppm (s, CH_3).

Bis(dimethylstibanyl)sulfane (**2**). Compound **2** was prepared as already described in the literature [18]. The yellow solid melts at 29 to 31 °C to give a colorless, mobile liquid (b. p. 65 °C/0.2 mbar).

NMR (benzene-d_6 solution). ^{1}H (200 MHz): 0.99 ppm (s, $^1J_{CH}$ = 133.5 Hz, CH_3); ^{13}C{^{1}H} (50 MHz): 5.70 ppm (s, CH_3).

We thank the Fonds der Chemischen Industrie, D-60329 Frankfurt, for financial support as well as *Prof. Dr. Th. Schleid*, Institut für Anorganische Chemie der Universität Stuttgart, *Prof. Dr. W. S. Sheldrick*, Lehrstuhl für Analytische Chemie der Ruhr-Universität Bochum, and *Prof. Dr. B. Engelen*, Fachbereich Chemie–Biologie der Universität–GH Siegen, for helpful discussions.

References

[1] H. J. Breunig, in S. Patai (ed), *The Chemistry of Organic Arsenic, Antimony and Bismuth Compounds*, Wiley, Chichester 1994, p. 441; G. Becker, O. Mundt, in B. Krebs (ed), *Unkonventionelle Wechselwirkungen in der Chemie metallischer Elemente*, VCH, Weinheim 1992, p. 199; A. Kuhnen, W. Müller-Warmuth, M. Prager, O. Mundt, M. Reti, G. Becker, *Z. Naturforsch.* **1997**, *A 52*, 306; G. Becker, J. Egner, M. Meiser, O. Mundt, J. Weidlein, *Z. Anorg. Allg. Chem.* **1997**, *623*, 941.

[2] a) R. M. Bozorth, *J. Am. Chem. Soc.* **1923**, *45*, 1621; b) K. E. Almin, A. Westgren, *Ark. Kemi* **1942**, *15 B*, 22/1; c) C. Svensson, *Acta Crystallogr.* **1975**, *B 31*, 2016.

[3] a) M. J. Buerger, St. B. Hendricks, *Z. Kristallogr.* **1938**, *98*, 1; b) C. Svensson, *Acta Crystallogr.* **1974**, *B 30*, 458.

[4] a) W. Hofmann, *Z. Kristallogr.* **1933**, *86*, 225; b) S. Šćavničar, *Z. Kristallogr.* **1960**, *114*, 85; c) P. Bayliss, W. Nowacki, *Z. Kristallogr.* **1972**, *135*, 308; d) N. V. Belov, Yu. G. Zagal'skaya, E. A. Pobedimskaya, *Dokl. Akad. Nauk SSSR* **1973**, *209*, 1330; *Sov. Phys. Dokl.* **1973**, *18*, 214; e) D. O. McKee, J. T. McMullan, *Z. Kristallogr.* **1975**, *142*, 447.

[5] K. Łukaszewicz, A. Pietraszko, J. Stepień-Damm, J. Grigas, A. Kajokas, *Pol. J. Chem.* **1997**, *71*, 390 and references cited therein.

[6] P. Arun, A. G. Vedeshwar, *J. Mater. Science* **1996**, *31*, 6507.

[7] J. S. Swinnea, A. J. Tenorio, H. Steinfink, *Am. Mineral.* **1985**, *70*, 1056.

[8] Kh. A. Mady, S. M. Hammad, W. Z. Soliman, *J. Mater. Science* **1987**, *22*, 4153.

[9] E. Diemann, *Z. Anorg. Allg. Chem.* **1977**, *433*, 242.

[10] L. Červinka, A. Hrubý, *J. Non-Crystalline Solids* **1982**, *48*, 231.

[11] A. Haaland, V. I. Sokolov, H. V. Volden, H. J. Breunig, M. Denker, R. Rösler, *Z. Naturforsch.* **1997**, *B 52*, 296.

[12] A. Haaland, D. J. Shorokhov, H. V. Volden, H. J. Breunig, M. Denker, R. Rösler, *Z. Naturforsch.* **1998**, *B 53*, 381.

[13] A. Haaland, D. J. Shorokhov, V. I. Sokolov, H. V. Volden, H. J. Breunig, M. Denker, R. Rösler, *Phosphorus, Sulfur, Silicon* **1998**, *136, 137 & 138*, 463.

[14] J. Zemann, *Kristallchemie*, Sammlung Göschen, Vol. 1220/1220 a, de Gruyter, Berlin 1966, p. 133.

[15] H. Krebs, *Grundzüge der anorganischen Kristallchemie*, Enke Verlag, Stuttgart 1968, p. 241 f.

[16] A. F. Wells, *Structural Inorganic Chemistry*, 5th ed., Clarendon Press, Oxford 1984, p. 889 and 907.

[17] G. T. Morgan, G. R. Davies, *Proc. Roy. Soc. London, Ser. A* **1926**, *110*, 523.

[18] H. J. Breunig, H. Jawad, *Z. Naturforsch.* **1982**, *B 37*, 1104.

[19] M. Dodd, St. L. Grundy, K. J. Reimer, W. R. Cullen, *Appl. Organomet. Chem.* **1992**, *6*, 207.

[20] H. J. Breunig, M. Jönsson, R. Rösler, E. Lork, *Z. Anorg. Allg. Chem.* **1999**, *625*, 2120.

[21] a) Th. Hahn (ed), *International Tables for Crystallography*, Vol. A *Space-Group Symmetry*, 2nd ed., Reidel Publ. Comp., Dordrecht (NL) 1984; b) J. A. Ibers, W. C. Hamilton (eds), *International Tables for X-ray Crystallography*, Vol. IV, Kynoch Press, Birmingham 1974, p. 47; c) N. Walker, D. Stuart, *Acta Crystallogr.* **1983**, *A 39*, 158; d) G. M. Sheldrick, *Program System SHELX-97*; University of Göttingen, Göttingen 1997; e) D. T. Cromer, J. B. Mann, *Acta Crystallogr.* **1968**, *A 24*, 321; D. T. Cromer, D. Liberman, *J. Chem. Phys.* **1970,** *53*, 1891; f) R. F. Stewart, E. R. Davidson, W. T. Simpson, *J. Chem. Phys.* **1965**, *42*, 3175; g) *DIAMOND – A Visual Crystal Structure Information System*, CRYSTAL IMPACT, Version 2.1c, Bonn 1999; h) *Program System SHELXTL Plus*, Revision 4.02, Siemens Analytical X-Ray-Instruments Inc., Madison, Wisconsin (USA) 1989.

---

[5] One should note that the aforementioned four-electron three-center bond changes to an at least eight-electron five-center bond, when the originally short sequence S1–Sb1··S2 is extended to S1–Sb1··S2–Sb2–S3 (no discrimination of symmetry-related atoms) and further weak interactions are quantum-chemically taken into account.

[22] J. Bordner, B. C. Andrews, G. G. Long, *Cryst. Struct. Commun*. **1974**, *3*, 53.

[23] M. Wieber, N. Graf, *Z. Anorg. Allg. Chem*. **1993**, *619*, 1991.

[24] R. E. DesEnfants, II, J. A. Gavney, Jr., R. K. Hayashi, A. D. Rae, L. F. Dahl, A. Bjarnason, *J. Organomet. Chem*. **1990**, *383*, 543.

[25] a) M. Bourgault, R. Fourcade, G. Mascherpa, *J. Solid State Chem*. **1981**, *36*, 214; b) R. L. Davidovich, L. A. Zemnukhova, A. A. Udovenko, L. V. Samarets, *Koord. Khim*. **1982**, *8*, 374.

[26] a) N. Wiberg, *Holleman-Wiberg – Lehrbuch der Anorganischen Chemie*, 101. ed., de Gruyter, Berlin 1995, p. 1838; b) *ibid*, p. 144; c) E. Wiberg, *Holleman-Wiberg – Lehrbuch der Anorganischen Chemie*, 81.–90. ed., de Gruyter, Berlin 1976, p. 128.

[27] a) I. D. Brown, *J. Solid State Chem*. **1974**, *11*, 214; J. Galy, G. Meunier, S. Andersson, A. Åström, *J. Solid State Chem*. **1975**, *13*, 142; M. Trömel, *J. Solid State Chem*. **1980**, *35*, 90; E. Philippot, *J. Solid State Chem*. **1981**, *38*, 26; I. D. Brown, *Acta Crystallogr*. **1992**, *B 48*, 553; X. Wang, F. Liebau, *Z. Kristallogr*. **1996**, *211*, 437; C. Preiser, J. Lösel, I. D. Brown, M. Kunz, A. Skowron, *Acta Crystallogr*. **1999**, *B 55*, 698; see also: D. V. Pushkin, V. N. Serezhkin, Yu. A. Buslaev, Yu. N. Mikhailov, *Zh. Neorg. Khim*. **1999**, *44*, 781; *Russ. J. Inorg. Chem*. **1999**, *44*, 721; b) X. Wang, F. Liebau, *Acta Crystallogr*. **1996**, *B 52*, 7; c) J. Olivier-Fourcade, P.-E. Lippens, J.-C. Jumas, M. Womes, I. Lefebvre, M. Lannoo, J.-M. Esteva, R. Karnatak, *Eur. J. Solid State Inorg. Chem*. **1993**, *30*, 139 and references cited therein.

[28] H. J. Breunig, M. A. Mohammed, K. H. Ebert, *Polyhedron*, **1994**, *13*, 2471.

[29] N. W. Alcock, *Adv. Inorg. Chem. Radiochem*. **1972**, *15*, 1.

[30] G. A. Landrum, R. Hoffmann, *Angew. Chem*. **1998**, *110*, 1989; *Angew. Chem. Int. Ed. Eng*. **1998**, *37*, 1887.

[31] J. K. Burdett, *Molecular Shapes – Theoretical Models of Inorganic Stereochemistry*, Wiley & Sons, New York 1980, p. 80 f.; J. K. Burdett, *Chem. Rev*. **1988**, *88*, 3; B. M. Gimarc, *Molecular Structure and Bonding – The Qualitative Molecular Orbital Approach*, Academic Press, New York 1979.

[32] K. H. Ebert, H. J. Breunig, C. Silvestru, I. Haiduc, *Polyhedron* **1994**, *13*, 2531.

[33] U. Müller, A. T. Mohammed, *Z. Anorg. Allg. Chem*. **1983**, *506*, 110.

[34] T. Bjorvatten, O. Hassel, A. Lindheim, *Acta Chem. Scand*. **1963**, *17*, 689.

[35] a) W. Lindemann, R. Wögerbauer, P. Berger, *Z. Anorg. Allg. Chem*. **1977**, *437*, 155; b) M. Schmidt, R. Bender, Ch. Burschka, *Z. Anorg. Allg. Chem*. **1979**, *454*, 160.

[36] G. R. Willey, M. T. Lakin, M. Ravindran, N. W. Alcock, *J. Chem. Soc., Chem. Commun*. **1991**, 271.

[37] A. F. Wright, M. S. Lehmann, *J. Solid State Chem*. **1981**, *36*, 371 and references cited therein.

[38] a) R. E. Gibbs, *Proc. Roy. Soc. London, Ser. A* **1927**, *113*, 351; b) M. Sato, *Mineral. J*. **1964**, *4*, 115; 131; c) K. Kihara, *Z. Kristallogr*. **1978**, *148*, 237 and references on tridymite cited therein.

[39] a) Cambridge Crystallographic Data Centre (ed), CSD Cambridge Structural Database, Cambridge (UK), Version 04/99; b) Fachinformationszentrum Karlsruhe (ed), ICSD Inorganic Crystal Structure Database, Karlsruhe, Version 1999/1.

[40] L. Yeo, K. D. M. Harris, *Acta Crystallogr*. **1997**, *B 53*, 822 and references cited therein.

[41] L. Mazzarella, C. Pedone, R. Puliti, *Acta Crystallogr*. **1973**, *B 29*, 2699.

[42] J. L. Calderon, F. A. Cotton, B. G. DeBoer, J. Takats, *J. Am. Chem. Soc*. **1971**, *93*, 3592.

[43] a) A. F. Wells, *J. Chem. Soc*. **1947**, 1662; b) A. W. Schlueter, R. A. Jacobson, R. E. Rundle, *Inorg. Chem*. **1966**, *5*, 277; c) A. G. Christy, R. J. Angel, J. Haines, S. M. Clark, *J. Phys.: Condens. Matter* **1994**, *6*, 3125.

[44] a) L. B. Asprey, F. H. Kruse, K. H. Jack, R. Maitland, *Inorg. Chem*. **1964**, *3*, 602; b) F. W. B. Einstein, P. R. Rao, J. Trotter, N. Bartlett, *J. Chem. Soc. A* **1967**, 478.

[45] B. Žemva, K. Lutar, A. Jesih, W. J. Casteel, Jr., A. P. Wilkinson, D. E. Cox, R. B. Von Dreele, H. Borrmann, N. Bartlett, *J. Am. Chem. Soc*. **1991**, *113*, 4192.

[46] F. A. Cotton, E. Babaian-Kibala, L. R. Falvello, M. Shang, *Inorg. Chem*. **1990**, *29*, 2591.

[47] R. Kniep, H. G. Will, I. Boy, C. Röhr, *Angew. Chem*. **1997**, *109*, 1052; *Angew. Chem. Int. Ed. Eng*. **1997**, *36*, 1013.

[48] J. Olivier-Fourcade, E. Philippot, M. Maurin, *Z. Anorg. Allg. Chem*. **1978**, *446*, 159.

[49] G. Cordier, C. Schwidetzky, H. Schäfer, *Rev. Chim. Minér*. **1982**, *19*, 179.

[50] W. S. Sheldrick, M. Wachhold, *Coord. Chem. Rev*. **1998**, *176*, 211.

[51] K.-J. Range, R. Leeb, *Z. Naturforsch*. **1975**, *B 30*, 889; Th. Schleid, *Z. Naturforsch*. **1992**, *B 47*, 45 and references cited therein.

[52] I. D. Brown in M. O'Keeffe, A. Navrotsky (eds), *Structure and Bonding in Crystals*, Vol. II, Academic Press, New York 1981, p. 1.

[53] A. Skowron, I. D. Brown, *Acta Crystallogr*. **1990**, *C 46*, 527; 531; 534.